Article

A New Procedure to Design an Open Circuit Blowing Subsonic Moist-Air Wind Tunnel

José A. Orosa [1,*] , Enrique J. García-Bustelo [1] and Diego Vergara [2]

1   Department of Nautical Science and Marine Engineering, Universidade da Coruña, Paseo de Ronda, 51, 15011 A Coruña, Spain; gbust@udc.es
2   Technology, Instruction, and Design in Engineering and Education Research Group (TiDEE.rg), Catholic University of Ávila, 05005 Ávila, Spain; diego.vergara@ucavila.es
*   Correspondence: jaorosa@udc.es

Featured Application: Moist air wind tunnels are an unknown tool to test, validate theoretical studies, and improve the design of wind turbines under different weather conditions.

Abstract: The present research work shows how a functional subsonic moist-air wind tunnel has been designed. Although this type of wind tunnel has never been developed to date, it is particularly interesting to develop a satisfactory design of feasibility under moist air conditions. Low-speed vertical-axis wind turbines employ different kinds of rotors, such as Savonius, Darrieus, and H-rotor. All these wind turbines present clear advantages, e.g., the horizontal-axis wind turbines are omnidirectional. This means they can work under different wind directions, need lower maintenance, and begin working under low wind speeds of 3 m/s. Recently, a new application of wind concentrators enabled the vertical-axis wind turbines to improve their performance coefficient based on new concepts like moist air phase change, which are being analysed to improve energy conversion. Thus, expectations were raised to design a suitable wind tunnel that accounts for the relative humidity of moist air. An initial prototype showed that the behaviour of open wind tunnels where the relative humidity of moist air was controlled by an adiabatic evaporative process was satisfactory. However, for such wind tunnels, certain improvements like computer control systems would need to be developed.

Keywords: wind energy; concentrator; low speed; moist air; experiment; CFD

1. Introduction

In the recent past, several engineers have evinced special interest in different engineering applications like wind tunnel tests for civil constructions and their effects on different structures [1,2]. Further, most of these wind tunnels were of the open-loop type [3]. However, on analysing the climatic environments, different outdoor regions were observed to present different weather conditions. Thus, interestingly, it was noted that not only did the outdoor air velocity influence wind energy conversion, but new parameters, including the relative humidity of moist air, also needed to be considered in the design and operation of such applications. Different relative humidity conditions of outdoor air in humid regions like that in Galicia (Spain) are listed in Figures 1–4 [4]. Such relative humidity clearly influences the flow of moist air, particularly affecting the density and enthalpy of moist air, as shown in Figure 5. Similarly, different applications were designed and employed in the case of dry air. Dry air is used in wind turbines, cars, planes and nearly all devices involving moist-air aerodynamics.

Europe is recognised as the world leader in wind energy, and many new regions will experience a definite increase in wind power installation once 100 MW wind generating capacity is achieved [5,6]. To analyse the behaviour of different wind turbines, wind tunnels and computational fluid dynamic (CFD) simulations need to be applied. Wind tunnels have commonly been described as equipment designed to obtain air-flow conditions to

simulate similar ambiences for comparative study [7]. In this context, several wind tunnels in the past were evaluated and developed, but none of them presented the moist air control system. Moist air needs to be assessed in conditions similar to real conditions in outdoor environments.

Generally, wind turbines are commonly associated with horizontal-axis wind turbines (HAWT). However, several new concepts need to be developed and understood when wind farms are designed in the future. Vertical-axis wind turbines (VAWT) are clearly more advantageous when compared with horizontal-axis wind turbines, which are omnidirectional, meaning they can work under different wind directions, require lower maintenance, and begin working under low wind speeds of 3 m/s. Just last year, a new application of wind concentrators enhanced the performance coefficient of the vertical-axis wind turbines.
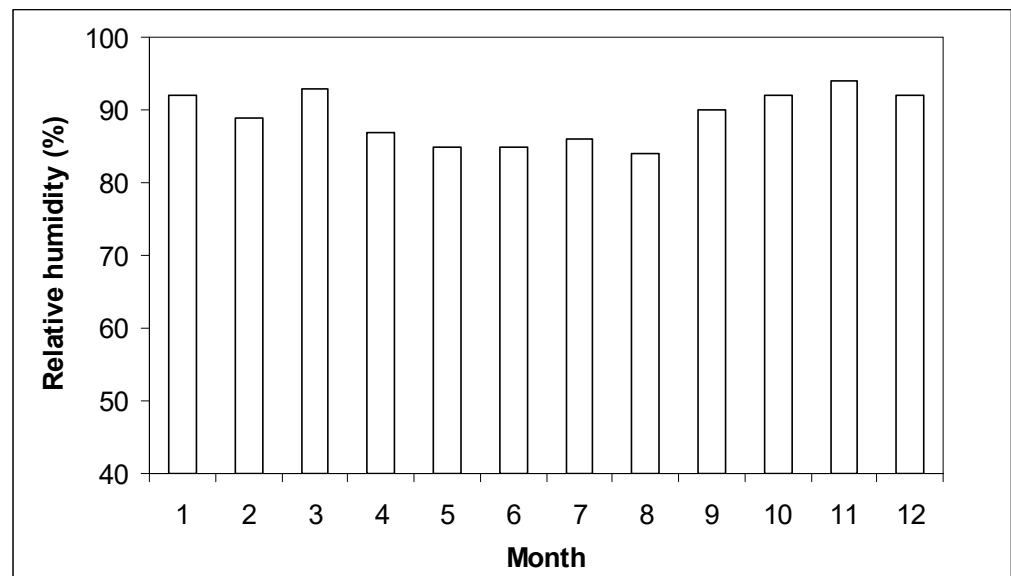

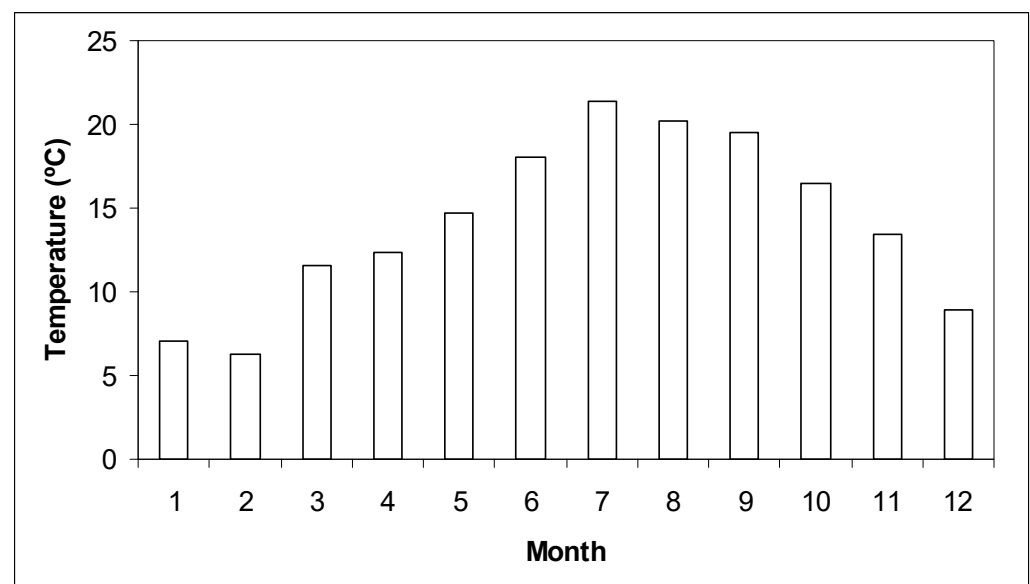**Figure 1.** Relative humidity of outdoor air in Galicia (Spain).

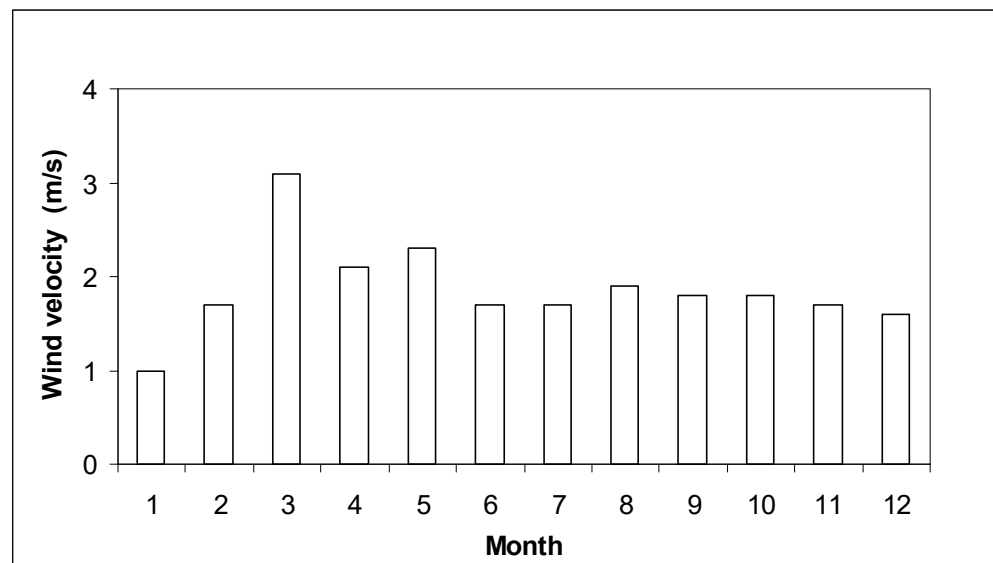**Figure 2.** Outdoor air temperature in Galicia (Spain).

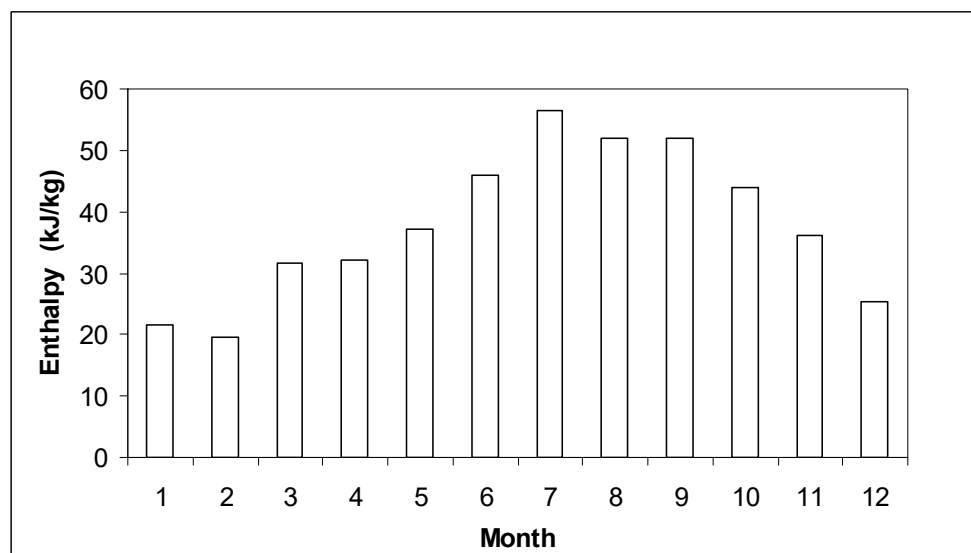**Figure 3.** Outdoor air velocity in Galicia (Spain).

Figure 4. Outdoor air enthalpy in Galicia (Spain).

From the beginning, for a VAWT with a typical Savonius rotor model, a convergent nozzle was used instead of the flat plate suggested by Sabzevan in 1977 [8]. What is more, increasing the power yield in relation to the rotor-swept concentrators is proposed [9], producing acceleration in the flow velocity by employing a diffuser duct and a funnel. In particular, the Savonius rotor is an example of a solution previously investigated [10,11]. Other researchers developed experiments to improve the performance of the Savonius wind rotor by curtain arrangement [12], leading to a power coefficient increase of 38.5%.

Furthermore, the advantages of VAWTs' blades and their attachments are that they have a lower cost, are more rugged in operation, and since most VAWT working parts that may require maintenance are placed at ground level, they will be easily accessible according to [13,14]. Finally, to implement VAWTs' wind energy conversion during low wind velocity, it is necessary to consider the conditions behind and in front of the converter [15].
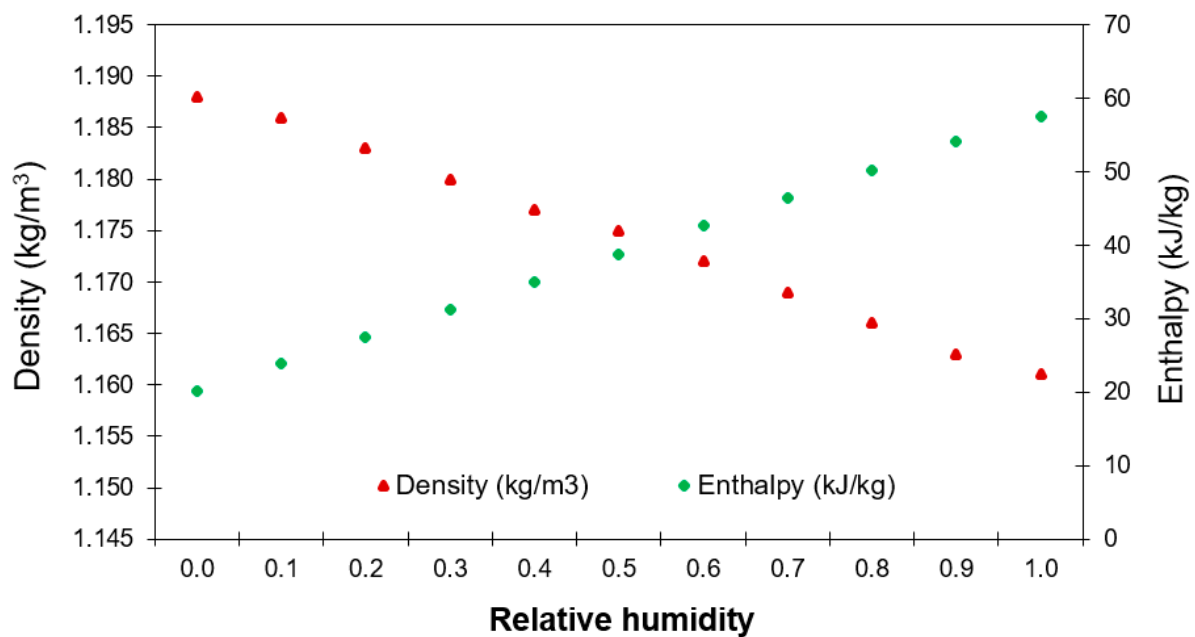
Figure 5. Relationship between relative humidity, enthalpy and density of moist air.

Based on these previous works [16], a vertical axis wind turbine concentrator design and test were set up considering one more parameter, the moist air density, as a fundamental way to increase wind turbine power conversion, showing that the wind concentrator was tested under different moist air densities and an input air velocity around 3 m/s. The experimental and simulated results show an increase in the velocity ratio whenever the air density is reduced. A posterior work [17] showed that, when their models were employed to the changed climatic conditions by the year 2030, it was concluded that the VAWT would be less affected by climate change than the HAWT. From these studies, it was concluded that there is a need to evaluate and optimise wind concentrator design and test with more complex wind tunnels. Now, new concepts, like moist air phase change, are being analysed to improve energy conversion. Therefore, designing an adequate wind tunnel that takes into account the relative humidity of moist air becomes particularly interesting.

Previous works analysed the effect of ice or humidity in wind tunnels [18,19], but none of them showed the way to empty this with a nozzle that causes the moist air phase change and its associated energy release. In this sense, relating the relative humidity of moist air to dry air becomes significant because different densities and energy are noted with each different relative humidity value. For example, to provide a reference for the power output of wind turbines, it is compared with the power of the free-air stream, which flows through the same cross-sectional area (A), according to Equation (1).

$$P_0 = \frac{1}{2} \cdot \rho \cdot v_1^3 \cdot A \tag{1}$$

where ρ is the moist air density (kg/m^3), v_1 is the wind velocity (m/s), and A is the cross-sectional area (m^2).

From this equation, wind turbine power conversion is observed to mainly depend on the cross-sectional area, moist air density and wind velocity. Hence, the properties of moist air will influence this energy conversion; however, this parameter was hardly ever taken into account in these processes. To consider this, wind velocity, as well as new parameters in weather conditions, like moist air properties, need to be analysed. Thus, if the total monthly wind energy is compared, the next figures can be arrived at. Figure 6 shows outdoor moist air temperature, relative humidity and its corresponding enthalpy. From this figure, it can be concluded that the outdoor moist air presents maximum enthalpy during the months between April and September as a clear function of outdoor air temperature

during the spring and summer seasons. However, Figure 7 shows the outdoor air velocity, density and corresponding kinetic energy. This kinetic energy, as seen, depends on the outdoor air velocity as it presents a cubic power value with respect to the density of moist air. Figure 7 thus shows that the kinetic energy is obtained from February to May.
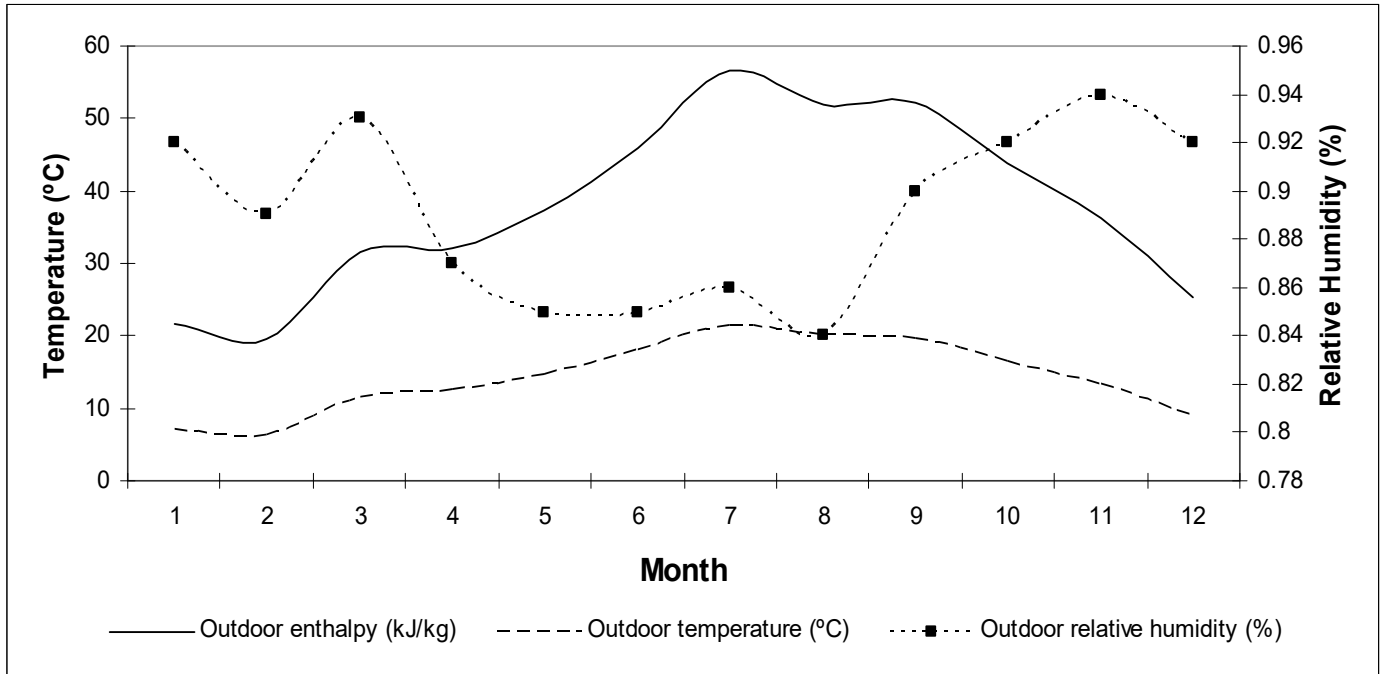

Figure 6. Outdoor air temperature, relative humidity and enthalpy.

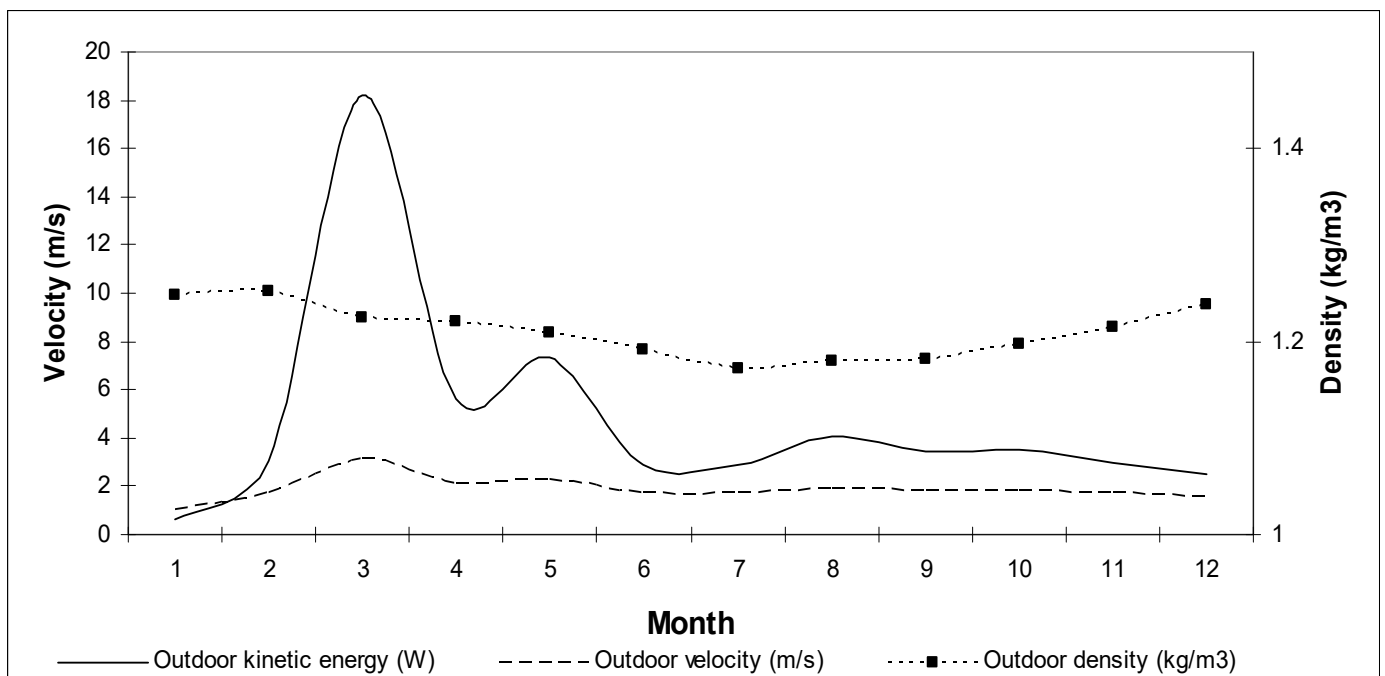**Figure 7.** Outdoor air density, velocity and kinetic energy.

Figures 6 and 7 show that the energy of moist air depends not only on the wind speed, as typically employed in wind turbines, but also on the design and operation of the wind farms. Fluid enthalpy particularly needs to be considered due to the total energy of the moist air, which has been summarised in these two points. From these Figures, outdoor air

enthalpy has been seen to depend on the temperature of the moist air. Additionally, the relative humidity of outdoor air exerts a lower influence, although it does not exert a phase change. Therefore, because of all these parameters, the kinetic energy is transformed under different moist-air conditions into an irregular monthly real wind farm power, as shown in Figure 8. Actually, Figure 8 corresponds to the same region whose weather conditions were shown earlier. Thus, it becomes evident that wind power exerts a maximum value during the period between January and March.
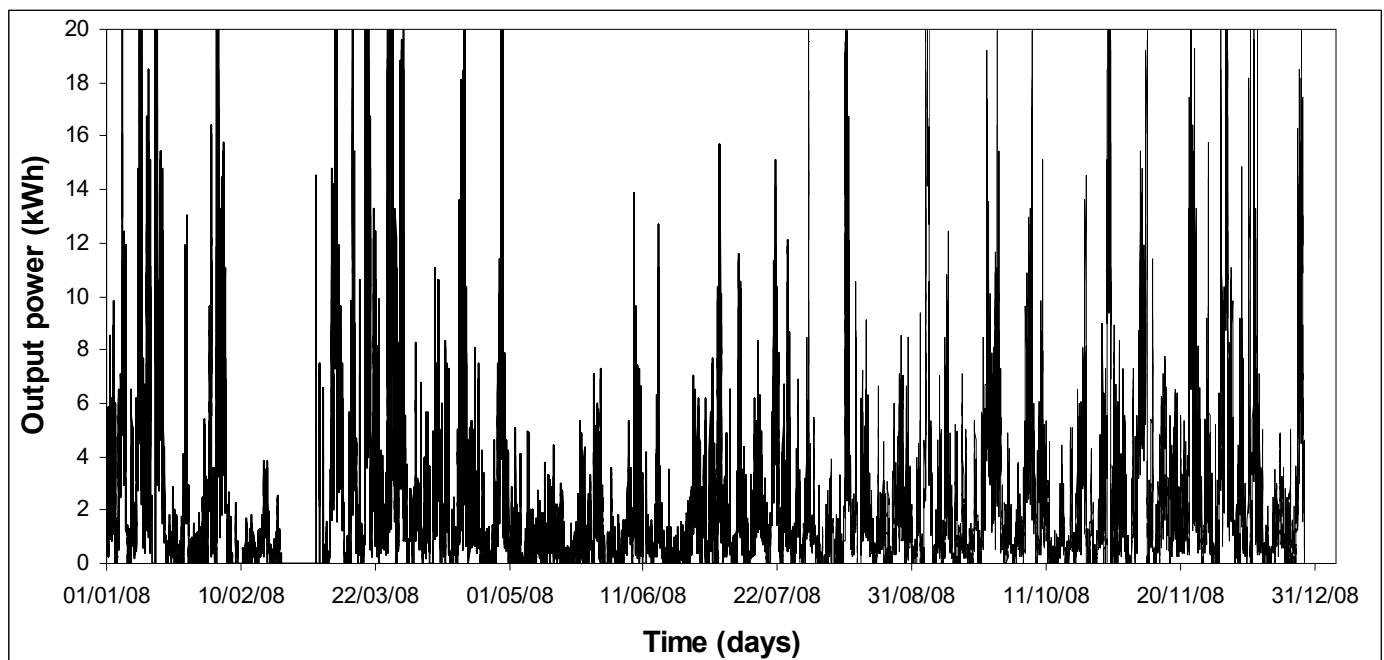
Figure 8. Real wind farm relationship between moist air and power output.

On studying the climatic conditions and the wind power conversion during the past years, it became interesting to set their relationship in real wind farms. To prove the truth, a 3D curve fit of a real sample was taken from a wind turbine farm power conversion considering the weather conditions of temperature, relative humidity and velocity. The first two parameters were expressed as moist-air density. Results proved an adequate model as a function of the cube of wind velocity for a correlation factor of 0.99, as shown in Equation (2).

$$P = -249,492.18 + 217,222.74 \cdot \rho + 1128.9655 \cdot V^3 \tag{2}$$

where p is the wind power production (kWh), and V is the wind velocity (m/s).

From this equation, and as shown earlier, it can be concluded that it is possible to obtain a constant power output throughout the year. To summarise, from the previous charts, it is evident that almost throughout the year, the energy of the outdoor moist air can be transformed into a constant power output in an adequate wind energy converter that takes into account the properties of moist air. Such a wind energy converter needs to be designed considering the total energy of moist air, and new design and testing tools for these new devices need to be improved in the future. In this paper, some software resources for these design improvements, like moist-air wind tunnels and computational fluid dynamics (CFD), are presented. Additionally, a real case study analysing the behaviour of the new moist-air wind concentrators is shown.

2. Materials and Methods

As mentioned earlier, the wind tunnel was designed in keeping with the study [7], in the same way as other authors did [13,14]. To reach test conditions, a control system for temperature, relative humidity and wind speed was employed. Measurements were

recorded by data loggers and a digital anemometer. The wind tunnel velocity was set at 5 m/s in accordance with other authors [5,20] who conducted a wind tunnel test in the range of 6 to 11 m/s.

Weather conditions of the region were sampled with climate stations located near the sampling site. Once the outdoor weather conditions were selected in line with the results of the climatic stations, they were simulated in the test room. Thus, the relative humidity of moist air was simulated using an adiabatic humidifier; the wind velocity was simulated with a ventilator; and finally, a settling chamber was used to obtain a laminar flow, as shown in Figure 9.
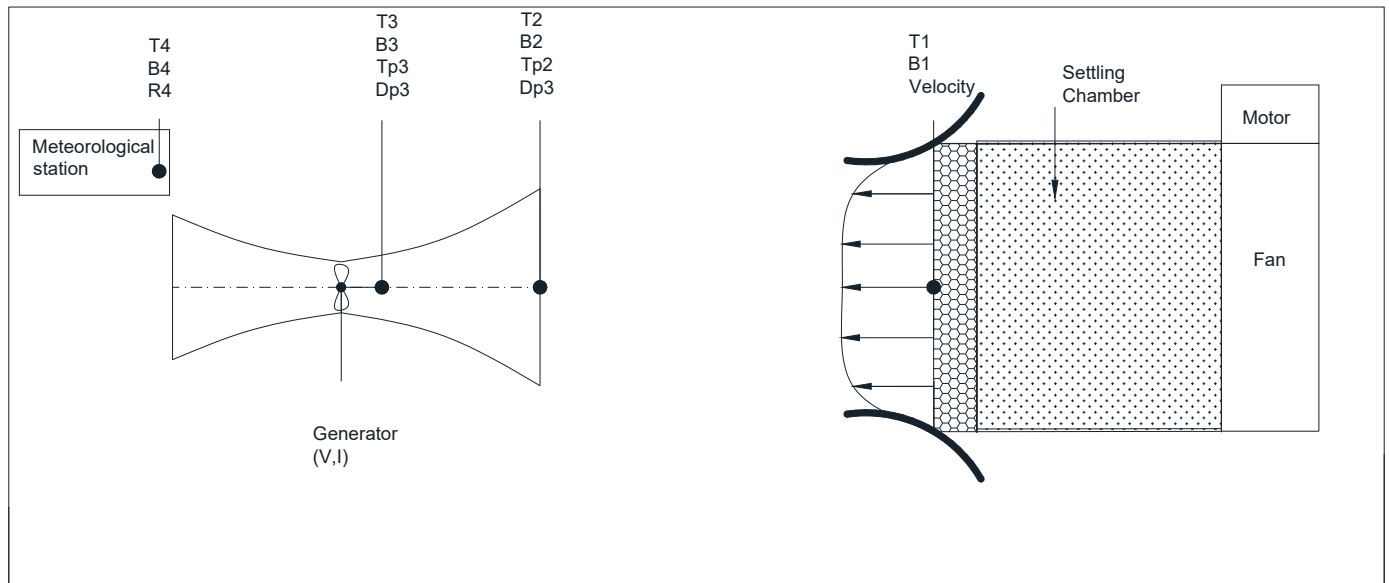
Figure 9. Schematic diagram of the experimental set-up and wind concentrator model.

In accordance with the earlier case studies, a wind tunnel that provides an adjustable air velocity between 0 and 10 m/s [21] has been designed. The wind tunnel is 8.3 m long. The test section is 1.2 m wide and 1.8 m long. A schematic diagram of the design process is shown in Figure 9 [22].

The EFD Lab software employs mass conservation, momentum conservation and energy conservation and has the advantage of evaluating the balance of condensed water vapour in the air-flow, correcting the corresponding changes that occur concerning temperature, density, enthalpy, specific heat and sonic velocity. The results obtained for humid air are valid when the fraction of condensed water does not exceed 5% by volume, and the temperature is in the range of 283 to 610 K. What is more, the CFD model employed in this research is based on boundary conditions that try to emulate wind velocity in outdoor ambiences and a convergence of the obtained results with sampled conditions in the outlet of the nozzle. Real fluids and friction were considered in these simulations. Finally, EFD lab employs automatic mesh generation and solver convergence controls that allow to take advantage of fully integrated flow simulation within the design cycle.

At the same time, the initial thermodynamic nozzle (wind concentrator) design consists of values for pressure, temperature, speed and relative humidity established in the nozzle inlet to define the geometry of the nozzle in accordance with a linear pressure drop.

It is important to highlight that the boundary chamber (room) was of dimensions that previous CFD simulations showed no interference with walls in any direction and ensured homogeneity of air-flow from the honeycomb. The main results, in agreement with wind tunnel design guides, it was obtained that a minimum of three times the dimension of the honeycomb must be the minimum distance to any wall to ensure no interference. It was validated with CFD simulations. What is more, the dimension of the boundary system was selected in accordance with some requirements, like that it must be reduced to get

a humidification level nearly constant in a relatively reasonable period of time (2 h, for instance) in agreement with the adiabatic saturation system capacities. These two main considerations were done, and iteratively, with CFD validations, let us define an adequate boundary environment for the dimension of our wind tunnel.

As the wind concentrator was designed to work with an outdoor air velocity of 5 to 10 m/s, these values were employed in the first simulations. As an asynchronous electrical motor had been used in the ventilator, the current frequency needed to be changed to define the different wind velocities. Such wind tunnels call for higher levels of relative humidity. Therefore, a relative humidity of 80 to 100% working range was selected, which is the typical value for outdoor climates in humid regions. Further, with this relative humidity of outdoor air, the moist-air phase change can be more easily reached.

As mentioned earlier, an automatic humidifier was employed to define the wind turbine power output under different relative humidity conditions of moist air. An adiabatic humidifier releases humidity to indoor air in an adiabatic process, taking the energy required to water phase change from the surrounding air, as shown in Figure 10. Therefore, the moist air will show an increase in relative humidity while the temperature of the moist air will be constant. Finally, different electrical heaters were placed in the room to control the temperature of moist air.

Figure 10. Adiabatic saturator (Spraying Systems Spain S.L. model 45,500).

To control and maintain the relative humidity of moist air, a test room was used to control the relative humidity of outdoor air. In this case study, a test room of an adequate length was chosen, which did not restrict air movement, with an adequate space between

the walls and the wind concentrator. Further, as a high level of relative humidity had been selected, most of the walls had been painted with impermeable paints.

Earlier research works [23] on wind tunnels with multiple fans employed oscillating blade rows to control the turbulence, indicating how it could be controlled by computers. In this case study, only a ventilator was needed with a settling chamber that allowed a laminar flow.

To generate the required air movement for each test, a Sodeca HPX-71-4T-3 ventilator with 2.2 kW 1400 rpm and a diameter of 70 cm was employed. This ventilator enabled us to develop a wind tunnel with air velocities between 0 and 10 m/s with a maximum flow of 24,000 m^3/h defined by frequency variation, as shown in Figure 11. However, to obtain a homogeneous air velocity, a honeycomb-structured setting chamber was employed, as shown in Figure 12. Finally, the rotor speed was measured using a digital tachometer having the least count of 1 rpm, and wind velocity at different sampling points to the test section was determined using a Pitot-static tube [20] Figure 13.

To define the power output, a wind turbine was located in the test section of the wind concentrator, as shown in Figure 14. Here, the power produced by the rotor was measured as the product of the force transmitted by the bucket and the bucket tip speed [21]. Similarly, this power can be defined using means of the voltage and the intensity of the current offered by a generator located in the shaft of the wind turbine. Further, to test the intensity, an electrical resistance of 330 ohms was employed to define the current intensity.

Figure 11. Ventilator and speed control system (Siemens Sinamics G110).

Figure 12. Test section (Honeycomb).

Figure 13. Anemometers.

Finally, to develop different designs of moist air processes, Engineering Equation Solver (EES) software was employed [16,24]. Similarly, to send information from data loggers to the computer and, consequently, to develop a real-time sampling process, the software LabView 6.0 [25] was employed with a target for real-time data acquisition. This option allows instantaneous values to be sent to a database like Microsoft Excel or Access and, from this application, develop different charts and statistical studies.
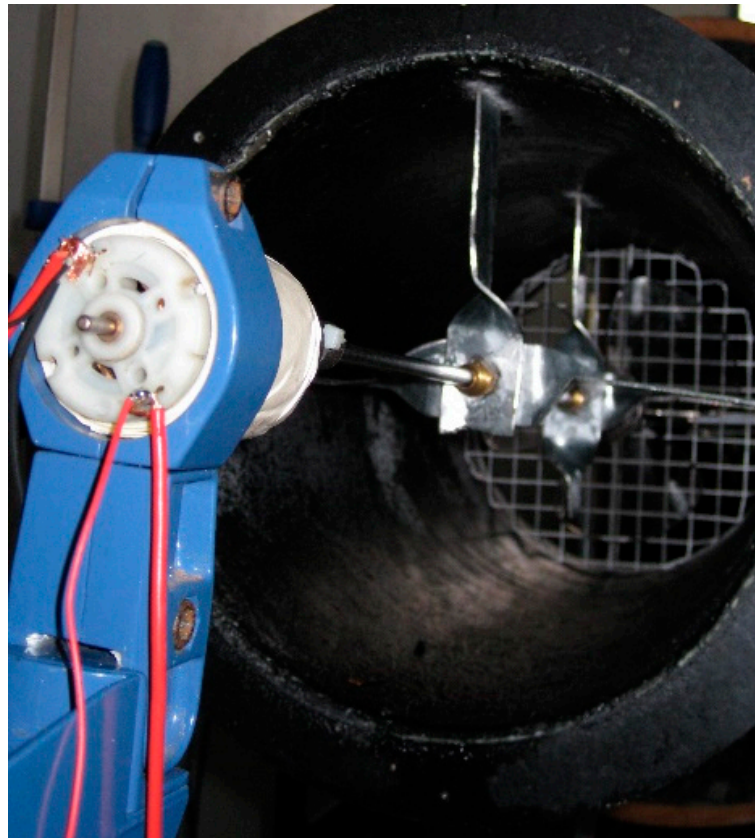
Figure 14. Wind generator.

3. A Practical Case Study of Moist-Air Wind Tunnel: Wind Concentrator Design

The wind concentrator has been designed considering the moist-air properties and, particularly, phase changes in the nozzle section [26,27]. Further, a second section that would act like a diffuser to restart the pressure in keeping with the surrounding ambience was added. Finally, a second ventilator could be employed to generate a clear depression in this final section of the wind concentrator with the aim of obtaining a laminar air-flow.

3.1. Real Sampled Data

Some authors [3] revealed that the flow in a wind tunnel test section must follow different standards to obtain accurate and reliable measurement data. Further, good air flow was observed to maintain a temporal steadiness of velocity and pressure reflected by the new indices that were developed. However, most of these indices were developed for closed-circuit wind tunnels, and no changes have been incorporated for open wind tunnels with moist-air properties. Thus, there is a paucity of information on this subject.

In line with the earlier sample data, a wind concentrator was developed based on an adiabatic and constant pressure drop process. To define this process, it must be understood that when the ambience air mass is introduced into the nozzle, mass and energy conservancy laws must be considered. Material conservancy can be defined as an internal flux under steady-state conditions, as shown in Equation (3).

$$\rho_1 \cdot A_1 \cdot V_1 = \rho_2 \cdot A_2 \cdot V_2 \qquad (3)$$

Similarly, energy conservation can be represented by Bernoulli's law for incompressible flows as well as compressible ones moving at low Mach numbers (Equation (4)).

$$\frac{P_2 - P_1}{\rho} + \frac{1}{2} \cdot \left(V_2^2 - V_1^2 \right) + g \cdot (z_2 - z_1) = 0 \qquad (4)$$

where p is the absolute fluid pressure (Pa), z is the height of the point above the reference plane (m), g is the acceleration due to gravity (m/s^2), and sub-indexes 1 and 2 represent the entrance and exit conditions. Adjusting these equations to the particle case of a nozzle and considering the ideal gas under constant specific heat, Equation (5) is arrived at:

$$V_2 = \sqrt{2 \cdot (T_1 - T_2) \cdot cp + V_1^2} \tag{5}$$

where T is the fluid temperature (K), cp is the specific heat.

Finally, if specific heat is introduced in Equation (5) and this equation is employed between two nozzle points, Equation (6) can be obtained.

$$\frac{T_2}{T_1} = \left(\frac{P_2}{P_1} \right)^{\frac{k-1}{k}} \tag{6}$$

where

$$k = \frac{cp}{cv} \tag{7}$$

$$cv = cp - R \tag{8}$$

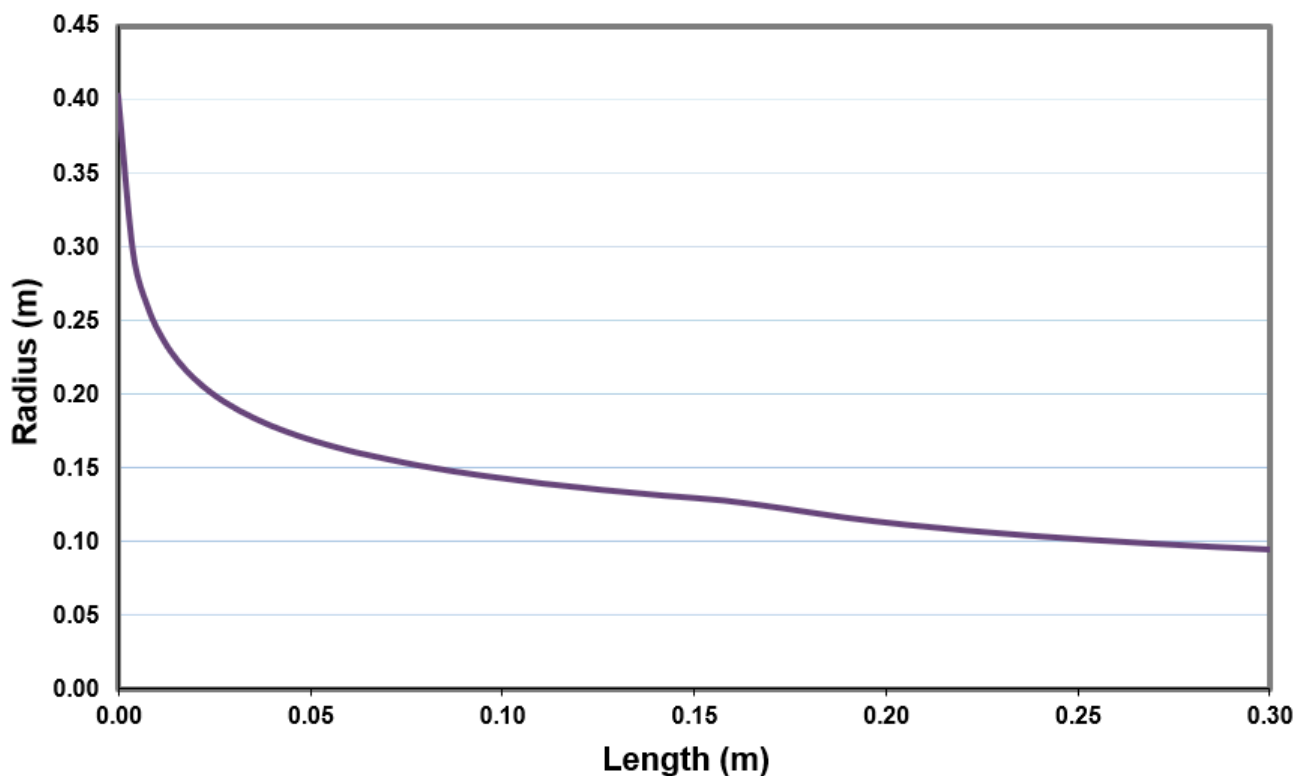The main results were plotted in Figure 15, showing wind concentrator dimensions.

Figure 15. The mathematical solution of wind concentrator shape.

Basically, the moist air in the nozzle will reach a higher partial vapour pressure due to this pressure drop together with the kinetic energy transformation. Further, this practical case study aimed to prove that the moist-air phase change can accelerate energy conversion. Thus, a prototype of this wind concentrator was developed. To this end, a fibre coat saturated with polyester resin materials was employed (Figure 16). This type of material was selected because it helped reduce the heat energy transfer from the nozzle to the outdoor air, reaching a higher possible approach to an adiabatic process. This kind of material was used to reduce the temperature of the moist air and to achieve adequate

moist-air phase change under a new lower pressure within the wind concentrator. Different conclusions were arrived at from such simulations. For example, an average decrease of 0.6 °C in temperature from the inlet (point 2) to the minimal sectional area (point 3) was obtained.
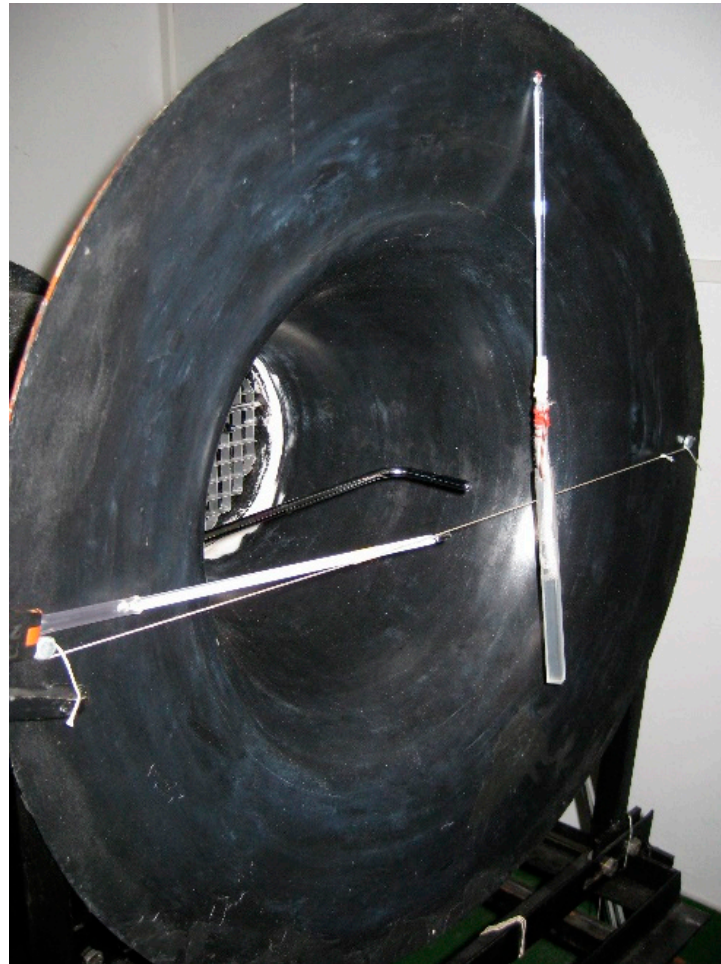
Figure 16. Prototype of wind concentrator.

This wind concentrator was then painted to reduce the external roughness. The margin of error of the sampled moist air values is 3% of relative humidity, and an increment of 1 m/s in moist air velocity was employed. Further, its different measurement, the hot wire turbulence intensities in the empty tunnel showed a uniform velocity anemometer was calibrated.

3.2. Analysis of Performance of a Wind Rotor

To define the real performance of a wind rotor, some authors have defined this parameter using the relationship between the power coefficient (C_p) versus tip-speed ratio (λ) and the torque coefficient (C_t) versus tip-speed ratio (λ) under different overlap ratio conditions.

$$C_p = \frac{P_{rotor}}{\left(\frac{1}{2}\rho \cdot A \cdot V_1^2\right)} \tag{9}$$

$$u = \left(\frac{1}{2}\rho \cdot A \cdot V_1^2\right)\frac{\pi DN}{60} \tag{10}$$

$$\tau = \frac{60 \cdot P}{2 \cdot \pi \cdot N} \tag{11}$$

$$C_t = \frac{\tau}{\frac{1}{2}\rho \cdot A \cdot V_1^2 \cdot d} \tag{12}$$

$$\lambda = \frac{u}{V} \tag{13}$$

where d is the bucket diameter of the rotor, D is the overall rotor diameter, P_{rotor} is the power output from the rotor, τ represents the torque, ρ; is the density, N is the r.p.m, u is the velocity of the tip of the blade, V is the free stream velocity, V_1 represents the velocity at the inlet to the test section, λ is the tip-speed ratio (TSR).

This coefficient was considered to define the performance under different moist-air conditions. Other constructive parameters are shown in Figure 17, like the constant e, which represents the overlap.
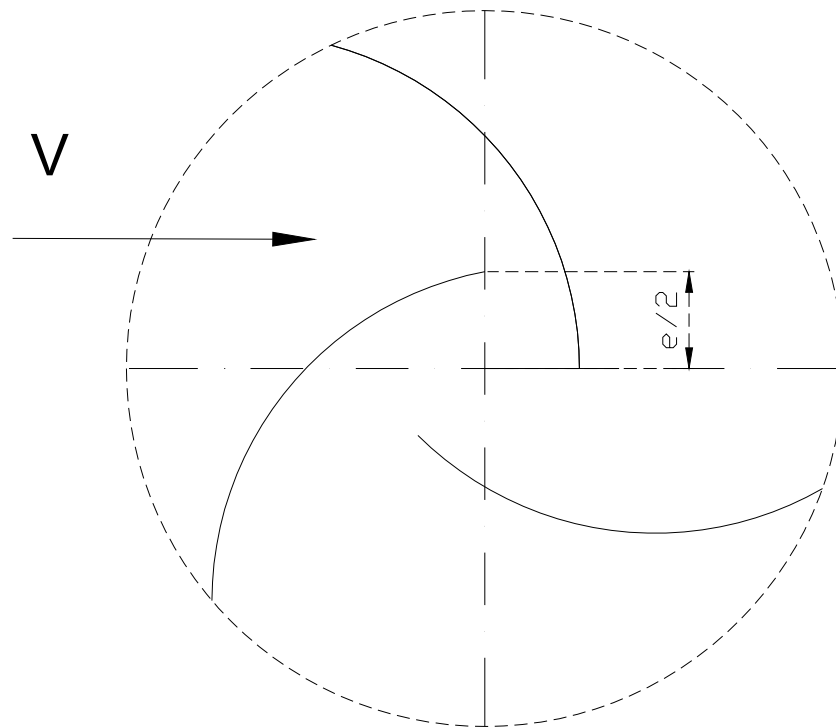
Figure 17. Three-bucket Savonius rotor.

To employ this equation, the overlap ratio must be understood, which is defined as the ratio of overlap to the overall rotor diameter, as shown in Figure 17. This equation shows the performance coefficient in such case studies.

4. Results

4.1. Wind Concentrator

As in previous research works, velocity and turbulence intensity measurements in the empty tunnel showed uniform field and low turbulence intensity. Measurements were taken by a sampling process with respect to the centre line of the air stream coming from the settling chamber. These measurements were developed every 10 cm and with respect to the centre point in the diagonal, horizontal and vertical axes. This information belongs to a basic initial test of the settling chamber in accordance with the general indications about test chamber design and test. In particular, it was identified the variation ratio of wind velocity from the centre line.

Finally, the open wind tunnel clearly proved to offer adequate performance once developed following this methodology. Once the wind concentrator was developed, it was tested under different wind tunnel conditions of temperature and relative humidity. Particularly, the values $T = 19\,°C$ and the relative humidity values of 55%, 75%, 90% and 95%

that corresponded with test numbers 2, 3, 4 and 5 were selected, as shown in Figures 18–20. Test 1 defined steady-state conditions.
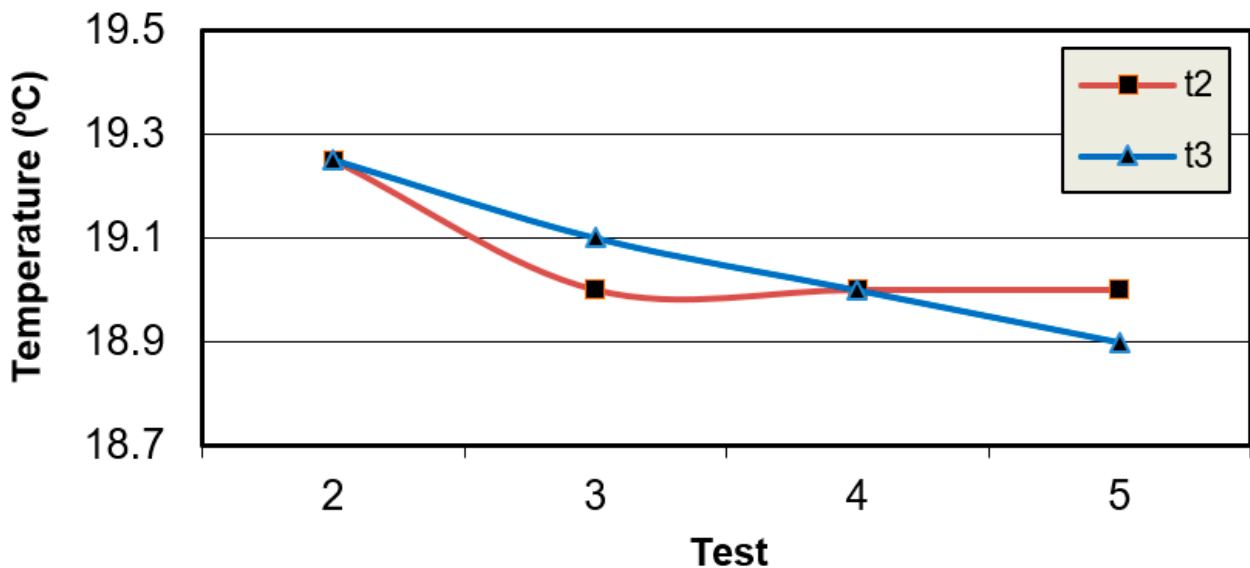

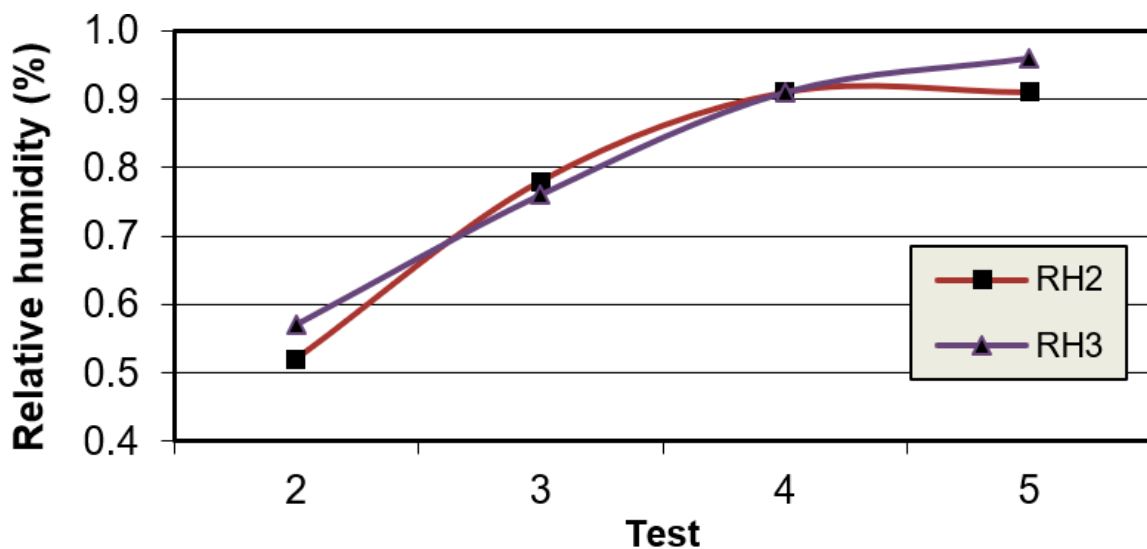**Figure 18.** Wind concentrator sampled temperature (°C).

Figure 19. Wind concentrator sampled relative humidity (%).

These figures showed a temperature decrease of 0.3 °C between the nozzle inlet temperature (point 2) and the nozzle output conditions (point 3), as seen in Figure 18. Similarly, a pressure decrease of 5 Pa, which implied an increase of 5% relative humidity of moist air, was obtained, as shown in Figure 19. However, the higher the relative humidity, the lower the moist air velocity was, in point 3, as 100% of the relative humidity of moist air and moist air phase change was never reached, see Figure 20. It is related to the temperature and density of moist air.

4.2. CFD Simulations

CFD simulations were performed using the EFD lab 8.0 software, as it is one of the few software resources that simulate moist air conditions. These simulations were validated with real data samples. For example, the influence of walls on air-flow within a room can be defined and, consequently, if the final room dimensions are sufficient. Further, new

parameters like wall paints and adiabatic processes can be considered. Moist air flow is not influenced by the temperature conditions of the walls.

A 3D model of the wind concentrator was developed, as shown in Figure 21, and it was simulated under the same weather conditions as the real case study. The results are revealed in Figures 22–25. Following this, the air velocities in points 1, 2 and 3 at different wind velocities were simulated, and the main results are listed in Figure 26.
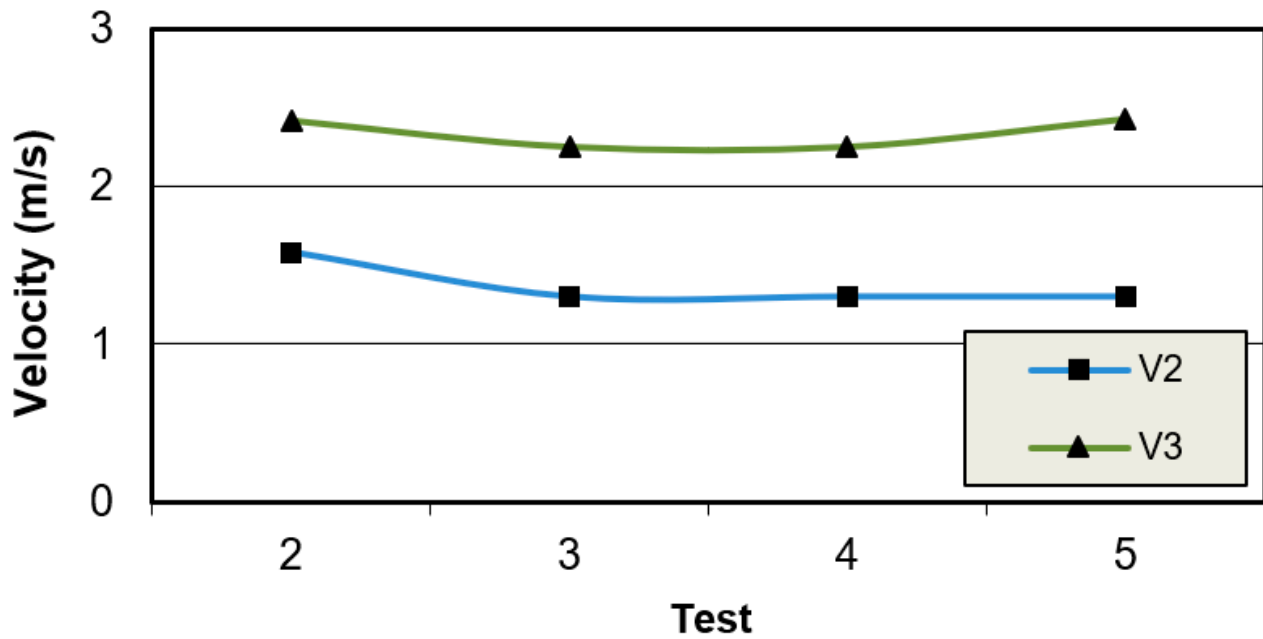
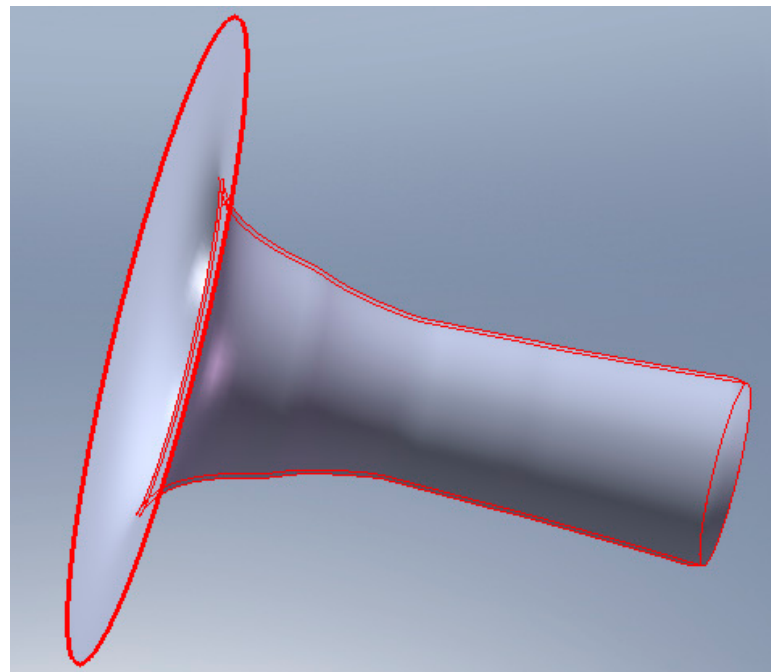**Figure 20.** Wind concentrator sampled velocity (m/s).
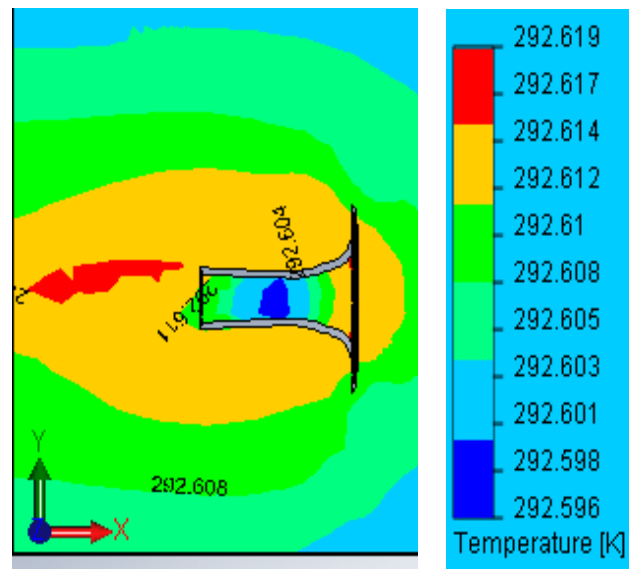
Figure 21. 3D wind concentrator design.

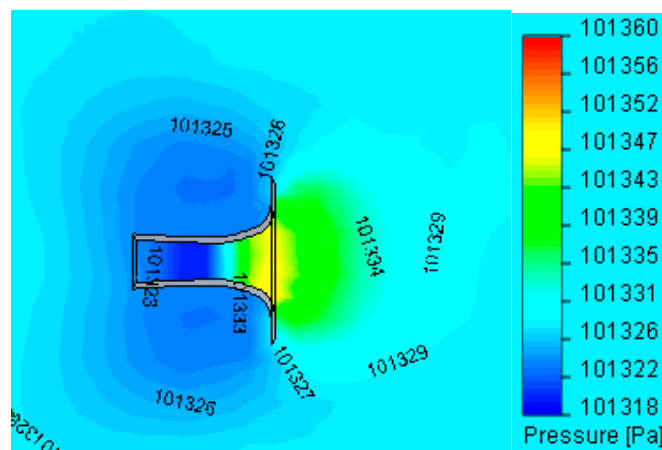**Figure 22.** Moist air temperature (m/s): *RH* = 95%, *p* = 101,328 Pa, *V* = 5 m/s.

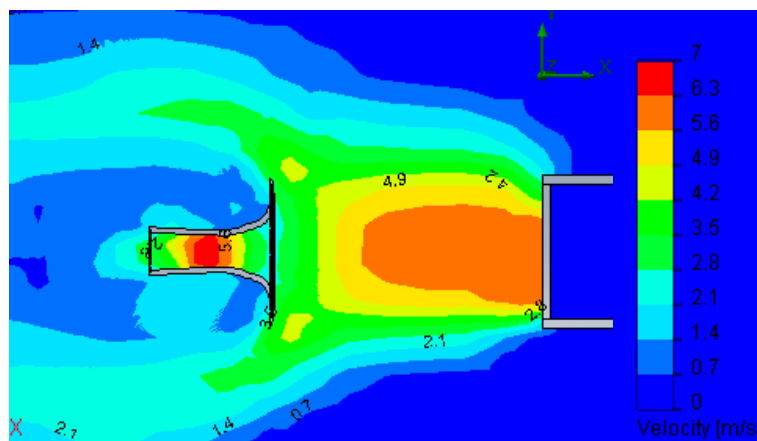**Figure 23.** Moist air pressure (m/s): *RH* = 95%, *p* = 101,328 Pa, *T* = 292.8 K, *V* = 5 m/s.

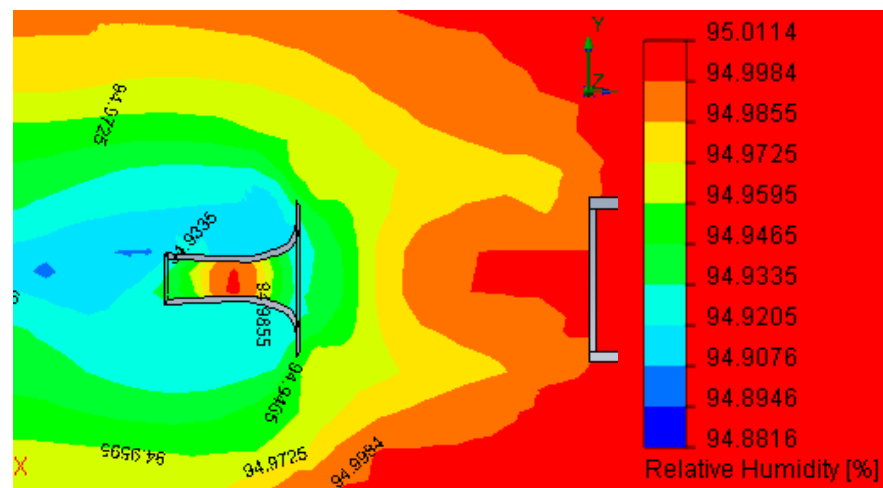**Figure 24.** Moist air velocity (m/s): *RH* = 95%, *p* = 101,328 Pa, *T* = 292.8 K, *V* = 5 m/s.

Figure 25. Moist air relative humidity (m/s): *p* = 101,328 Pa, *T* = 292.8 K, *V* = 5 m/s.
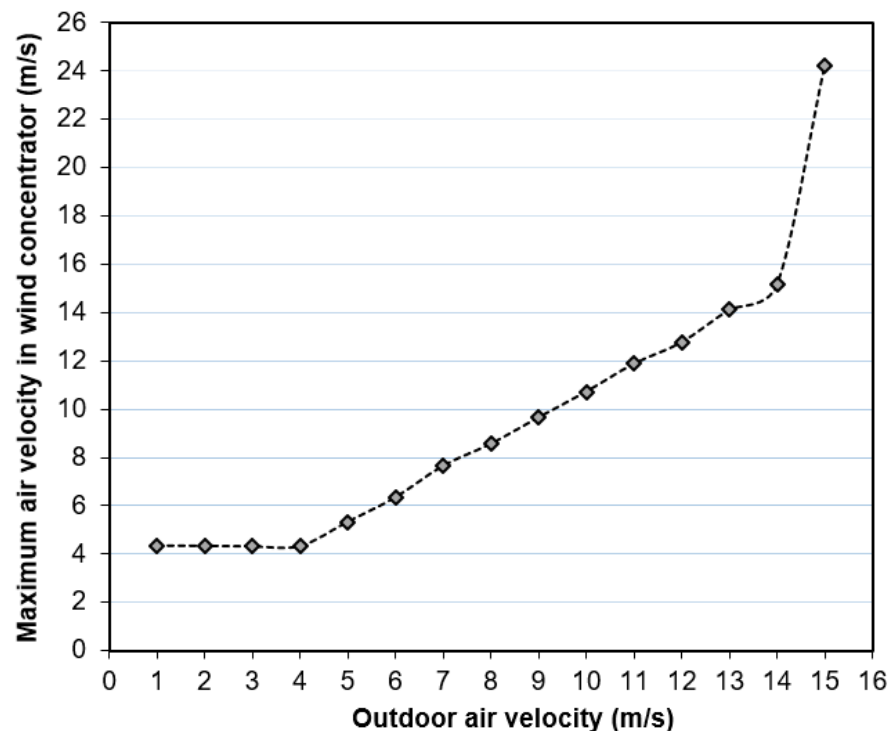

Figure 26. Simulation of wind concentrator velocity (point 3) at 100%.

5. Discussion

In the present paper, a moist-air wind tunnel prototype that revealed the real behaviour of moist-air phase change in a real wind concentrator under low wind velocities has been designed and developed. The wind tunnel was designed according to the study in [7], similar to the one in [13,14]. To reach the test conditions, temperature, relative humidity and wind speed control systems were used. Measurements were recorded using the data loggers and a digital anemometer. The wind tunnel velocity was set at 5 m/s in keeping with other authors [20,28] who had conducted a wind tunnel test in the range of 6 to 11 m/s.

This wind tunnel control system threw much light on the behaviour of wind concentrators and wind turbines under different weather conditions. Similarly, a new wind concentrator control system enabled the control of moist-air conditions at the inlet of the wind turbine and thus in energy conversion. However, some improvements, like computer control systems, must be developed for such types of wind tunnels.

In consequence, this system may be a laboratory test that emulates the behaviour of a low-speed wind turbine that receives moist air from a nozzle that improves the wind energy conversion based on the moist air phase change. In this sense, point 1 of Figure 9 represents the wind and points 2 and 3 let us understand the real conditions in the nozzle inlet (point 2) and nozzle throat (point 3). Furthermore, in Figures 18–20, an expansion process that makes a reduction in moist air temperature and an increase in the relative humidity when reaching from point 2 to point 3. These results were validated with CFD simulations, which are shown in Figures 22–25, but, as it can be appreciated, in accordance with the nozzle design, the 3D distribution of the relative humidity and temperature is not homogeneous in each point but getting an average value in agreement with sampled data.

It must be highlighted that the phase change process was obtained partially when the weather conditions reached 95% (something so common during the night in some Galician regions in the winter season). In consequence, although in point 3, an increase in moist-air velocity was updated, sampled data showed that this increase was not as high as expected. This is because the energy released from moist air depends on its phase change, and it can only be reached when the relative humidity is 100% in this section. This need for 100% relative humidity inside the nozzle implies an outdoor air relative humidity of 98%, which is a too high value for an open wind tunnel based on adiabatic saturation of the air. Despite this, 98% of relative humidity can be obtained in humid areas in outdoor conditions in the Galician winter season during certain periods of time.

Once the CFD simulations were validated with the average value of the prototype, it is possible to understand what may happen if 100% of relative humidity is obtained inside the nozzle by more simulations. In consequence, an outdoor air velocity was simulated at 100% in this situation, as shown in Figure 26.

From Figure 26, it is evident that this model, in accordance with its original design, shows a clear increase in moist-air velocity in the lower section from 5 m/s of outdoor air. It also reveals a constant proportionality value with respect to the outdoor air from 5 to 14 m/s. From this last value, a really significant increase to 24 m/s was obtained.

The sensibility at the time to sample moist air pressure in Pa proved to be really complicated due to electronic devices not letting us be accurate enough, and differential manometers were needed (certified by the calibration certificate by the seller). The number of decimal points employed to sample this variable was adequate to sample inlet and outlet conditions of air in the nozzle. Despite this, the pressure during the moist air condensation process could not be sampled, and simulations, as it was explained in the CFD model description, were limited to 5% despite the fact that a higher condensation may occur. This effect could only be demonstrated by the increase in air velocity at the outlet of the nozzle.

In consequence, this energy conversion is not the maximum energy that can be obtained from this energy converter due to the limitations of the CFD software. This is because the CFD software can simulate 5% of the moisture condensation and not more inclusive if the phase change continues. Indeed, a clear higher condensation is expected that may happen if the nozzle-wind turbine system is placed in an adequate outdoor Galician place and, consequently, a higher energy conversion. Further, it is one of the few CFD software that simulates moist air condensation. This is another point to be improved in the future.

Finally, in conclusion, to reach the same values as in simulations, an indoor air relative humidity of 95% or higher must be reached to obtain moist-air condensation in the nozzle. This is a very difficult objective to achieve. This can be obtained only with a high investment in humidifiers and distilled water. Finally, real field studies must be developed in the future to validate the wind tunnel results.

To summarise, it can be concluded that real moisture conditions need to be thoroughly analysed. Further, if these conditions need to be analysed in a test chamber like a moist air wind tunnel, then CFD simulations [29], particularly the energy release with a condensation phase change, must be performed [30]. All these parameters must be analysed in future research works.

6. Conclusions

In the present paper, some original results were obtained:

1. A moist air wind tunnel prototype that revealed the real behaviour of moist-air phase change in a real wind concentrator under low wind velocities was designed and developed.
2. Experimental results showed that this energy conversion was not the maximum energy that can be obtained from this energy converter because moist air condensation is not reached, and consequently, an improvement in the moist-air humidification process and software resources are required.
3. CFD Simulations showed that energy release with a condensation phase change warrants greater energy release, improving the energy conversion in wind farms.

Author Contributions: Conceptualisation, J.A.O.; methodology, J.A.O. and E.J.G.-B.; validation, E.J.G.-B. and D.V.; formal analysis, J.A.O.; data curation, E.J.G.-B. and D.V.; writing—original draft preparation, J.A.O.; writing—review and editing, J.A.O. and D.V. All authors have read and agreed to the published version of the manuscript.

Institutional Review Board Statement: Not applicable.

Informed Consent Statement: Not applicable.

Data Availability Statement: Not applicable.

Conflicts of Interest: The authors declare no conflict of interest.

References

1. Bowen, A.J. Modeling of strong wind flows over complex terrain at small geographic scales. *J. Wind. Eng. Ind. Aerod.* **2003**, *91*, 1859–1871. [CrossRef]
2. Cermak, J.E. Wind tunnel development and trends in applications to civil engineering. *J. Wind. Eng. Ind. Aerod.* **2003**, *91*, 355–370. [CrossRef]
3. Moonen, P.; Blocken, B.; Carmeliet, J. Indicators for the evaluation of wind tunnel test section flow quality and application to a numerical closed-circuit wind tunnel. *J. Wind. Eng. Ind. Aerod.* **2007**, *95*, 1289–1314. [CrossRef]
4. MeteoGalicia. *Galicia Climatic Data 2007*; Consellería de Medio Ambiente; Xunta de Galicia: Santiago de Compostela, Spain, 2007.
5. Herbert, G.M.J.; Iniyan, S.; Sreevalsan, E.; Rajapandian, S. A review of wind energy technologies. *Renew. Sust. Energ. Rev.* **2007**, *11*, 1117–1145. [CrossRef]
6. El-Naggar, M.; Sayed, A.; Elshahed, M.; El-Shimy, M. Optimal maintenance strategy of wind turbine subassemblies to improve the overall availability. *Ain Shams Eng. J.* **2023**, *14*, 102177. [CrossRef]
7. Wittwer, A.R.; Möller, S.V. Characteristics of the low-speed wind tunnel of the UNNE. *J. Wind Eng. Ind. Aerod.* **2000**, *84*, 307–320. [CrossRef]
8. Sabzevan, A. Performance characteristics of concentrator augmented Savonius wind rotors. *Wind Eng.* **1977**, *1*, 198–206.
9. Hau, E. *Wind Turbines: Fundamentals, Technologies, Application, Economics*, 2nd ed.; Springer: Berlin/Heidelberg, Germany, 2006.
10. Kamoji, M.A.; Kedare, S.B.; Prabhu, S.V. Performance test on helical Savonius rotors. *Renew. Energy* **2008**, *34*, 521–529. [CrossRef]
11. Irabu, K.; Roy, J.N. Characteristics of wind power on Savonius rotor using a guide-box tunnel. *Exp. Therm Fluid Sci.* **2007**, *32*, 580–586. [CrossRef]
12. Altan, B.D.; Atilgan, M.; Özdamar, A. An experimental study on improvement of Savonius rotor performance with curtaining. *Exp. Therm. Fluid Sci.* **2008**, *32*, 1673–1678. [CrossRef]
13. Shikha, A.N.; Bhatti, T.S.; Kothari, D.P. A New Vertical axis wind rotor using convergent nozzles. In Proceedings of the Large Engineering Conference on Power Engineering, Montreal, QC, Canada, 7–9 May 2003; pp. 177–181.
14. Shikha, S.; Bhatti, T.S.; Kothari, D.P. Air concentrating nozzles: A promising option for wind turbines. *Int. J. Energy Technol. Policy* **2005**, *3*, 394–412. [CrossRef]
15. van Bussel, G.J.W. The science of making more torque from wind: Diffuse experiments and theory revisited. *J. Phys. Conf. Ser.* **2007**, *75*, 012010. [CrossRef]
16. Orosa, J.A.; García-Bustelo, E.J. Low speed wind concentrator for wind farm power generation improvement. In Proceedings of the Industrial Electronics 2009, IECON'09, 35th Annual Conference of IEEE, Porto, Portugal, 3–5 November 2009; pp. 3605–3608. [CrossRef]
17. Orosa, J.A.; García-Bustelo, E.J.; Oliveira, A.C. Realistic solutions for wind power production with climate change. *Energy Sources Part A Recovery Util. Environ. Eff.* **2012**, *34*, 912–918. [CrossRef]

18. Li, Y.; Tagawa, K.; Feng, F.; Li, Q.; He, Q. A wind tunnel experimental study of icing on wind turbine blade airfoil. *Energy Convers. Manag.* **2014**, *85*, 591–595. [CrossRef]

19. Obligado, M.; Bayoán Cal, R.; Brun, C. Wind turbine wake influence on the mixing of relative humidity quantified through wind tunnel experiments. *J. Renew. Sustain. Energy* **2021**, *13*, 023308. [CrossRef]

20. Saha, U.K.; Rajkumar, M.J. On the performance analysis of Savonius rotor with twisted blades. *Renew. Energy* **2006**, *31*, 1776–1788. [CrossRef]

21. Gupta, R.; Biswas, A.; Sharma, K.K. Comparative study of a three-bucket Savonius rotor with a combined three-bucket Savonius–three-bladed Darrieus rotor. *Renew. Energ.* **2008**, *33*, 1974–1981. [CrossRef]

22. Chu, C.-R.; Wang, Y.-W. The loss factors of building openings for wind-drive ventilation. *Build. Environ.* **2010**, *45*, 2273–2279. [CrossRef]

23. Nishi, A.; Kikugawa, H.; Matsuda, Y.; Tashiro, D. Turbulence control in multiple-fan wind tunnels. *J. Wind. Eng. Ind. Aerod.* **1997**, *67–68*, 861–872. [CrossRef]

24. Moran, M.J.; Shapiro, H.N.; Boettner, D.D.; Bailey, M.B. *Fundamentals of Engineering Thermodynamics*, 8th ed.; Wiley: Hoboken, NJ, USA, 2014.

25. Faraco, G.; Gabriele, L. Using LabVIEW for applying mathematical models in representing phenomena. *Comput. Educ.* **2007**, *49*, 856–872.

26. Orosa, J.A.; García-Bustelo, E.J.; Oliveira, A.C. An experimental test of low speed wind turbine concentrators. *Energy Sources Part A Recovery Util. Environ. Eff.* **2012**, *34*, 1222–1230. [CrossRef]

27. Costa, A.M.; Bouzón, R.; Vergara, D.; Orosa, J.A. Eco-friendly pressure drop dehumidifier: An experimental and numerical analysis. *Sustainability* **2019**, *11*, 2170. [CrossRef]

28. Saha, U.K.; Thola, S.; Maity, D. Optimum design configuration of Savonius rotor through wind tunnel experiments. *J. Wind. Eng. Ind. Aerod.* **2008**, *96*, 1359–1375. [CrossRef]

29. Li, T.; Qu, H.; Zhao, Y.; Honerkamp, R.; Yan, G.; Chowdhury, A.; Zisis, I. Wind effects on dome structures and evaluation of CFD simulations through wind tunnel testing. *Sustainability* **2023**, *15*, 4635. [CrossRef]

30. Solaun, K.; Cerdá, E. Impacts of climate change on wind energy power—Four wind farms in Spain. *Renew. Energy* **2020**, *145*, 1306–1316. [CrossRef]